JOURNAL OF SOLID STATE CHEMISTRY 115, 76–82 (1995)

Hydrothermal Synthesis and Structure of $Mn_2VO(PO_4)_2 \cdot H_2O$

A. Mar, F. Leroux, D. Guyomard, A. Verbaere, and Y. Piffard[1]

Institut des Matériaux, Laboratoire de Chimie des Solides, UMR 110 CNRS-Université de Nantes, 2 rue de la Houssinière, 44072 Nantes Cedex 03, France

Received April 19, 1994; in revised form July 12, 1994; accepted July 15, 1994

Manganese(II) vanadyl phosphate hydrate, $Mn_2VO(PO_4)_2 \cdot H_2O$, has been prepared hydrothermally and characterized structurally from single crystal-diffraction data. It crystallizes in space group $P2_1/c$ of the monoclinic system with $Z = 4$ in a cell of dimensions $a = 8.957(2)$ Å, $b = 8.806(2)$ Å, $c = 9.329(2)$ Å, and $\beta = 100.95(1)°$. The outstanding feature of the structure is a tetrameric cluster of $Mn(1)O_5$ polyhedra and VO_6 octahedra. These clusters are linked together by $Mn(2)O_5$ polyhedra and PO_4 tetrahedra to yield the three-dimensional arrangement of the structure. The compound decomposes at 400°C to afford a nominally dehydrated phase. Magnetic susceptibility measurements confirm the assignment of the metal oxidation states as Mn(II) and V(IV) in the title compound. © 1995 Academic Press, Inc.

INTRODUCTION

In the course of ongoing investigations of the design of structures built up from octahedral and tetrahedral building blocks, we have embarked on the synthesis of new mixed transition-metal phosphates. Despite intense activity in the general area of transition-metal phosphates for many years, we have found no examples of any mixed manganese/vanadium phosphates, except for one recently reported compound, $[Mn(H_2O)]_{0.25}(VO)_{0.75}PO_4 \cdot 2H_2O$ (1). A great number of manganese phosphates are known, these having largely been discovered as minerals. Similarly, many vanadium phosphates have been prepared recently, partly motivated by interest in them as potential catalytic materials (2). Our interest in mixed manganese/vanadium systems stems from the possibility that both Mn and V can display, or can be made to exhibit (through electrochemical methods) mixed valency, and as such their compounds may serve as potential battery materials (3). We report here the preparation under hydrothermal conditions of the new compound $Mn_2VO(PO_4)_2 \cdot H_2O$, its crystal structure, and its thermal and magnetic properties.

[1] To whom correspondence should be addressed.

EXPERIMENTAL

Synthesis. Crystals of $Mn_2VO(PO_4)_2 \cdot H_2O$ were prepared by hydrothermal synthesis. A mixture of $H_2Mn_4O_9 \cdot xH_2O$ (rancieite) (414 mg, 1.0 mmole), $VOSO_4 \cdot 5H_2O$ (506 mg, 2.0 mmole), H_3PO_4 (10 mmole, 1.0 *M*), and 1,4-diazabicyclo[2.2.2]-octane (DABCO) (219 mg, 2.0 mmole), was placed in a Teflon vessel which was filled to a degree of 80% with water (final pH 1) and enclosed in a stainless steel bomb. We have shown previously that the use of rancieite (4) as a starting material is attractive because it is a phyllomanganate that is highly reactive (5). Its formula was calculated from TGA measurements to obtain the degree of hydration and from redox back titration measurements to obtain the Mn oxidation state. The mixture was heated at 180°C under autogenous pressure for 1 week, affording amber crystals in the shape of square plates containing Mn, V, and P in an atomic ratio of 2 : 1 : 2, as revealed from a microprobe analysis on a scanning electron microscope. The yield was close to 100% with respect to the Mn and V starting contents. That a compound containing Mn(II) is obtained suggests that the protonated DABCO probably served as a reducing agent rather than as a template as was intended.

Structure determination. Analysis of Weissenberg photographs revealed monoclinic symmetry and gave preliminary cell parameters. From powder diffraction data collected on an INEL multidetector system ($\lambda(CuK\alpha_1) = 1.54056$ Å; Si standard), the cell parameters were refined. Table 1 lists observed and calculated interplanar distances and the intensities calculated from the crystal structure with the use of the program LAZY-PULVERIX (6). Single-crystal intensity data were collected at room temperature on a Siemens P4 diffractometer under the conditions given in Table 2. Data reduction, structure solution, and refinements were carried out with the use of programs in the SHELXTL PLUS package (7). The systematic absences ($h0l$, $l = 2n + 1$; $0k0$, $k = 2n + 1$) lead uniquely to the centrosymmetric space group $P2_1/c$. Conventional atomic scattering factors and anomalous dispersion cor-

0022-4596/95 $6.00

TABLE 1
X-ray Powder Diffraction Data for $Mn_2VO(PO_4)_2 \cdot H_2O$

hkl	d_{obs} (Å)	d_{calc} (Å)	I–I_0	*hkl*	d_{obs} (Å)	d_{calc} (Å)	I–I_0
100		8.794	8	$31\bar{1}$	2.806	2.806	17
011	6.351	6.348	100	130	2.783	2.784	22
110		6.222	5	$21\bar{2}$	2.751	2.761	14
$11\bar{1}$	5.497	5.502	7	$22\bar{2}$		2.751	60
002	4.576	4.580	7	$30\bar{2}$	2.711	2.714	9
012	4.064	4.063	7	$13\bar{1}$		2.710	7
120	3.935	3.937	13	$31\bar{2}$	2.594	2.594	10
$21\bar{1}$	3.860	3.860	26	311		2.537	9
$20\bar{2}$	3.513	3.524	12	$10\bar{4}$	2.327	2.326	14
$12\bar{1}$		3.510	20	$31\bar{3}$	2.271	2.270	12
$21\bar{2}$	3.272	3.272	7	$13\bar{3}$	1.998	1.998	18
022	3.174	3.174	21	$14\bar{2}$		1.971	6
$12\bar{2}$	3.119	3.120	7	204	1.889	1.889	11
220		3.111	6	$23\bar{4}$		1.766	6
300	2.931	2.931	22	340	1.760	1.760	8
$11\bar{3}$	2.899	2.899	15	430		1.760	6
013	2.884	2.885	18	134		1.719	7
122	2.867	2.867	91	$05\bar{2}$		1.644	6
221	2.832	2.832	22	$14\bar{4}$	1.599	1.599	10

rections were used (8). A numerical absorption correction was applied to the data (min/max trans. = 0.69/0.90). The positions of all non-H atoms were found by direct methods, and the structure was refined by least-squares methods. All atoms had reasonable bond-valence sums *V* (9, 10) (Mn(1), 2.1; Mn(2), 1.8; V, 4.0; P(1), 4.8; P(2), 4.7; O, 1.8–2.0), except for O(8), which at this stage was bonded only to Mn(2) and for which *V* was only 0.33. This suggested that O(8) belonged to a water molecule. Moreover, with the assumption of an oxidation state assignment of Mn(II) and V(IV), the requirement for charge balance in the formula implies missing positive charge. Although subsidiary electron density was clearly visible near O(8) in the difference Fourier map, the positions of the H atoms could not be resolved, suggesting that the water molecule may be rotationally disordered to some extent. Additional evidence for the existence of a water of hydration in the compound comes from the infrared spectrum, which clearly shows the presence of O–H stretching and bending vibrations, and from TGA measurements, which show a weight loss at 400°C corresponding roughly to the loss of one water molecule per formula unit. The final cycle of refinement on *F* included anisotropic thermal parameters and resulted in residuals of $R = 0.041$ and $R_w = 0.028$ (136 variables, 1617 reflections) with $I > 2\sigma(I)$. The final difference electron density map shows extrema of $(\Delta\rho)_{max} = 0.9$ and $(\Delta\rho)_{min} = -1.0$ e$^-$ Å^{-3}. Final values of the positional and thermal parameters are given in Tables 3 and 4. A list of structure amplitudes is available as supplementary material.

TABLE 2
Crystal Data and Intensity Collection for $Mn_2VO(PO_4)_2 \cdot H_2O$

Formula	$Mn_2VO(PO_4)_2 \cdot H_2O$
Formula mass (amu)	384.78
Space group	$P2_1/c$
a (Å)	8.957(2)
b (Å)	8.806(2)
c (Å)	9.329(2)
β (°)	100.95(1)
V (Å^3)	722.4(3)
Z	4
ρ_c (g cm^{-3})	3.54
μ(Mo*K*α) (cm^{-1})	51.7
Crystal dimensions	Plate, 0.07 × 0.07 × 0.02 mm
Radiation	Mo*K*α, λ = 0.71073 Å
Scan mode	ω
Scan range (°)	1.2 + $\Delta\theta(\alpha_1, \alpha_2)$
2θ limits (°)	2.0–70.0
Data collected	$-1 \le h \le 14$, $-1 \le k \le 14$, $-15 \le l \le 14$
No. of data collected	4252
No. of unique data	3190 (R_{int} = 0.019)
No. of unique data, with $I > 2\sigma(I)$	1617
No. of variables	136 (including anisotropic temperature factors)
$R(F)^a$	0.041
$R_w(F)^b$	0.028
GOF	1.11

[a] $R(F) = \sum \| |F_o| - |F_c| \| / \sum |F_o|$.
[b] $R_w(F) = [\sum w(|F_o| - |F_c|)^2 / \sum wF_o^2]^{1/2}$ with $w = 1/\sigma^2(F)$.

Physical measurements. Infrared spectra were obtained on a 20SCX FTIR spectrometer with the use of KBr pellets. Thermal measurements were made on a Perkin–Elmer TGS-2 thermogravimetric analyzer. Magnetic measurements were conducted on a Quantum De-

TABLE 3
Positional and Equivalent Isotropic Thermal Parameters for $Mn_2VO(PO_4)_2 \cdot H_2O$

Atom	Wyckoff position	*x*	*y*	*z*	U_{eq} (Å^2)[a]
Mn(1)	4*e*	0.2203(1)	0.0675(1)	0.3893(1)	0.0120(3)
Mn(2)	4*e*	0.1594(1)	0.7331(1)	0.1531(1)	0.0137(3)
V	4*e*	0.4267(1)	0.4967(1)	0.2298(1)	0.0069(2)
P(1)	4*e*	0.0733(2)	0.3461(2)	0.1501(2)	0.0074(4)
P(2)	4*e*	0.5268(2)	0.2479(2)	0.0097(2)	0.0066(4)
O(1)	4*e*	0.0450(4)	0.1624(5)	0.4820(4)	0.013(1)
O(2)	4*e*	0.0811(4)	0.8765(4)	0.3039(4)	0.010(1)
O(3)	4*e*	0.1374(5)	0.1971(4)	0.2121(4)	0.015(1)
O(4)	4*e*	0.3936(5)	0.0191(5)	0.2664(4)	0.015(1)
O(5)	4*e*	0.4045(4)	0.3464(4)	0.0608(4)	0.009(1)
O(6)	4*e*	0.1841(4)	0.4798(4)	0.1978(4)	0.009(1)
O(7)	4*e*	0.3606(4)	0.6512(4)	0.0568(4)	0.009(1)
O(8)	4*e*	0.1592(4)	0.5570(5)	0.5252(4)	0.016(1)
O(9)	4*e*	0.6208(4)	0.1677(4)	0.1415(4)	0.009(1)
O(10)	4*e*	0.4405(5)	0.3581(4)	0.3952(4)	0.012(1)

[a] U_{eq} is defined as one-third of the trace of the orthogonalized U_{ij} tensor.

TABLE 4
Anisotropic Thermal Parameters[a] (Å²) in $Mn_2VO(PO_4)_2 \cdot H_2O$

Atom	U_{11}	U_{22}	U_{33}	U_{12}	U_{13}	U_{23}
Mn(1)	0.0099(4)	0.0148(4)	0.0112(4)	−0.0009(4)	0.0021(4)	−0.0013(4)
Mn(2)	0.0129(5)	0.0130(4)	0.0155(4)	0.0024(4)	0.0032(4)	−0.0032(4)
V	0.0076(4)	0.0066(4)	0.0063(4)	0.0006(4)	0.0011(3)	0.0000(4)
P(1)	0.0068(7)	0.0078(7)	0.0077(6)	−0.0005(6)	0.0013(5)	0.0009(6)
P(2)	0.0077(7)	0.0056(6)	0.0069(6)	0.0020(6)	0.0027(5)	0.0003(6)
O(1)	0.012(2)	0.017(2)	0.010(2)	0.004(2)	0.003(2)	0.001(2)
O(2)	0.009(2)	0.012(2)	0.010(2)	0.000(1)	0.003(2)	0.000(2)
O(3)	0.012(2)	0.014(2)	0.018(2)	0.003(2)	0.002(2)	0.004(2)
O(4)	0.009(2)	0.021(2)	0.014(2)	0.003(2)	0.002(2)	−0.001(2)
O(5)	0.008(2)	0.011(2)	0.009(2)	0.002(2)	0.003(2)	−0.001(2)
O(6)	0.007(2)	0.009(2)	0.010(2)	−0.003(2)	−0.001(1)	−0.002(2)
O(7)	0.010(2)	0.008(2)	0.010(2)	−0.000(2)	0.006(2)	0.002(2)
O(8)	0.013(2)	0.018(2)	0.016(2)	−0.004(2)	0.004(2)	−0.001(2)
O(9)	0.009(2)	0.009(2)	0.010(2)	0.003(2)	0.002(2)	0.005(2)
O(10)	0.016(2)	0.008(2)	0.011(2)	0.003(2)	0.003(2)	0.006(2)

[a] The form of the anisotropic thermal parameter is: $\exp[-2\pi^2(h^2a^{*2}U_{11} + k^2b^{*2}U_{22} + l^2c^{*2}U_{33} + 2hka^*b^*U_{12} + 2hla^*c^*U_{13} + 2klb^*c^*U_{23})]$.

sign SQUID magnetometer with the use of powdered samples (~20 mg) that were first cooled to 5 K at zero field and then warmed to 300 K under an applied field of 5 kOe. The data were corrected for contributions from sample holder background and core diamagnetism.

RESULTS AND DISCUSSION

Description of the structure. The compound $Mn_2VO(PO_4)_2 \cdot H_2O$ crystallizes in a new structure type. As it is relatively complex, the structure is best examined in parts, beginning with the coordination polyhedra. Table 5 lists bond distances and angles around various coordination polyhedra, which are shown in Fig. 1.

The Mn(1) polyhedra is (5 + 1)-coordinated. If only the five shortest Mn–O distances are considered (Fig. 1a), it can be described in two ways. In the trigonal bipyramidal description, O(1) and O(4) serve as the apical atoms, subtending an angle of 166.6(2)° around Mn(1), while O(2), O(3), and O(5) lie in the equatorial plane. Alternatively, in the square pyramidal description, O(3) at the axial position forms the shortest bond, 2.030(4) Å, to Mn(1), while O(1), O(2), O(4), and O(5) form longer bonds at the basal positions. Neither of these descriptions is wholly adequate, for the angular distortions are severe, and it is best to regard the coordination as intermediate between trigonal bipyramidal and square pyramidal. Completing the coordination sphere, O(7) forms a long sixth bond at 2.642(4) Å, which though weak is nonnegligible for it contributes 0.10 vu to the bond-valence sum of Mn(1) (cf. 0.51–0.33 vu for the other Mn(1)–O bonds of 2.030(4)–2.203(4) Å). The Mn(2) polyhedron, also (5 + 1)-coordinated, is even more highly distorted (Fig. 1c).

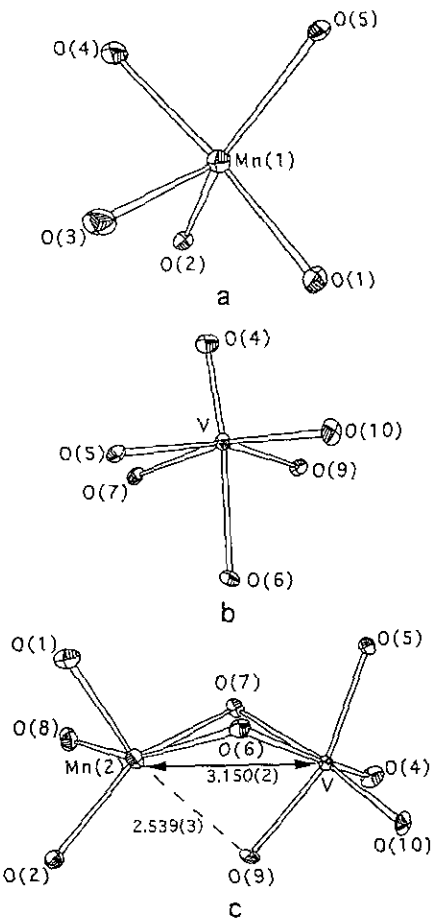

FIG. 1. Views of coordination environments in $Mn_2VO(PO_4)_2 \cdot H_2O$, showing the labeling scheme and 50% thermal ellipsoids for the atoms. (a) $Mn(1)O_5$ polyhedron, intermediate between a trigonal bipyramid and a square pyramid. (b) VO_6 octahedron. (c) $Mn(2)O_5$ polyhedron, sharing an edge with the VO_6 octahedron and forming a long sixth bond to O(9); the metal–metal distance is indicated.

TABLE 5
Selected Interatomic Distances (Å) and Angles (°) in $Mn_2VO(PO_4)_2 \cdot H_2O$

$Mn(1)O_6$ polyhedron

Mn(1)	O(1)	O(2)[a]	O(3)	O(4)	O(5)[b]	O(7)[c]
O(1)	2.104(4)	3.067(5)	2.813(6)	4.216(6)	3.164(5)	3.918(6)
O(2)[a]	92.1(2)	2.154(4)	3.021(6)	3.148(6)	4.177(5)	3.106(5)
O(3)	85.7(2)	92.4(1)	2.030(4)	2.746(6)	3.674(5)	4.615(5)
O(4)	166.6(2)	94.3(2)	82.3(2)	2.141(4)	2.976(5)	3.159(5)
O(5)[b]	94.5(1)	146.9(1)	120.4(2)	86.5(1)	2.203(4)	2.712(5)
O(7)[c]	110.8(1)	80.0(1)	161.9(2)	81.9(1)	67.4(1)	2.642(4)

$Mn(2)O_6$ polyhedron

Mn(2)	O(1)[d]	O(2)	O(6)	O(7)	O(8)[e]	O(9)[f]
O(1)[d]	2.110(4)	3.287(5)	2.881(5)	3.583(6)	3.068(6)	4.466(5)
O(2)	102.4(2)	2.107(4)	3.792(5)	4.209(6)	2.878(6)	3.202(5)
O(6)	82.1(1)	119.9(1)	2.272(4)	2.701(6)	4.376(6)	2.654(5)
O(7)	109.4(1)	147.3(1)	72.8(1)	2.278(4)	3.122(6)	2.792(5)
O(8)[e]	90.7(1)	83.8(2)	156.1(1)	88.4(1)	2.200(4)	4.136(5)
O(9)[f]	147.6(1)	86.6(1)	66.7(1)	70.6(1)	121.4(1)	2.539(3)

VO_6 polyhedron

V	O(4)[f]	O(5)	O(6)	O(7)	O(9)[f]	O(10)
O(4)[f]	1.615(4)	2.660(5)	3.749(6)	2.746(5)	2.847(6)	2.709(6)
O(5)	92.7(2)	2.040(4)	2.805(6)	2.712(5)	4.001(5)	3.077(5)
O(6)	172.7(2)	84.2(1)	2.141(4)	2.701(6)	2.654(5)	2.865(5)
O(7)	94.1(2)	81.6(1)	78.9(1)	2.108(4)	2.792(5)	4.035(5)
O(9)[f]	102.5(2)	160.5(1)	79.2(1)	85.1(1)	2.021(4)	2.789(5)
O(10)	98.4(2)	100.8(2)	88.7(2)	167.1(2)	89.2(2)	1.953(4)

$P(1)O_4$ tetrahedron

P(1)	O(1)[g]	O(2)[h]	O(3)	O(6)
O(1)[g]	1.542(4)	2.497(6)	2.479(5)	2.494(5)
O(2)[h]	107.9(2)	1.547(4)	2.497(6)	2.541(6)
O(3)	109.1(2)	109.9(2)	1.503(4)	2.532(5)
O(6)	107.5(2)	110.3(2)	112.0(2)	1.550(4)

$P(2)O_4$ tetrahedron

P(2)	O(5)	O(7)[i]	O(9)	O(10)[g]
O(5)	1.542(4)	2.551(6)	2.498(5)	2.434(5)
O(7)[i]	110.7(2)	1.558(4)	2.472(5)	2.528(5)
O(9)	109.1(2)	106.6(2)	1.525(4)	2.555(5)
O(10)[g]	105.5(2)	110.7(2)	114.4(2)	1.515(4)

Note. Symmetry code: (*a*) $x, y - 1, z$ (*b*) $x, -y + 1, z + 0.5$ (*c*) $x, -y + 0.5, z + 0.5$ (*d*) $-x, y + 0.5$, (*e*) $x, -y + 1.5, z - 0.5$ (*f*) $-x + 1, y + 0.5, -z + 0.5$ (*g*) $x, -y + 0.5, z - 0.5$ (*h*) $-x, y - 0.5, -z + 0.5$ (*i*) $-x + 1, -y + 1, -z$.

The O(6) and O(8) atoms lie at the axial positions, subtending an angle of only 156.1(1)°, in the trigonal bipyramidal description, while the O(1) atom lies at the apical position in the square pyramidal description. The weakly bound sixth atom O(9) at 2.539(3) Å contributes 0.13 vu to Mn(2) (cf. 0.42–0.27 vu for the other Mn(2)–O bonds of 2.107(4)–2.278(4) Å). The V polyhedron is a distorted octahedron (Figs. 1b and 1c) with one short bond (1.615(4) Å) to the vanadyl oxygen O(4) and five longer ones (1.953(4)–2.141(4) Å) to the other oxygen atoms. The $P(1)O_4$ and $P(2)O_4$ tetrahedra have P–O bond lengths (⟨P(1)–O⟩ = 1.536(5) and ⟨P(2)–O⟩ = 1.535(5) Å) typical of those found in other phosphates. The shortest P–O distances (P(1)–O(3) = 1.503(4) Å and P(2)–O(10) = 1.515(4) Å) correspond to oxygen atoms that are bonded to only two cations whereas the three other oxygen atoms of each PO_4 are bonded to three cations.

As shown in Fig. 2, the most distinctive feature of the structure is a cyclic tetrameric cluster of Mn(1) and V polyhedra. The role of the Mn(2) polyhedron will be considered later. Within this cluster, the $Mn(1)O_5$ and VO_6 polyhedra share corners through O(4) and O(5). Additionally, the metal polyhedra are clasped together through corner-sharing by $P(1)O_4$ tetrahedra at the ends of the

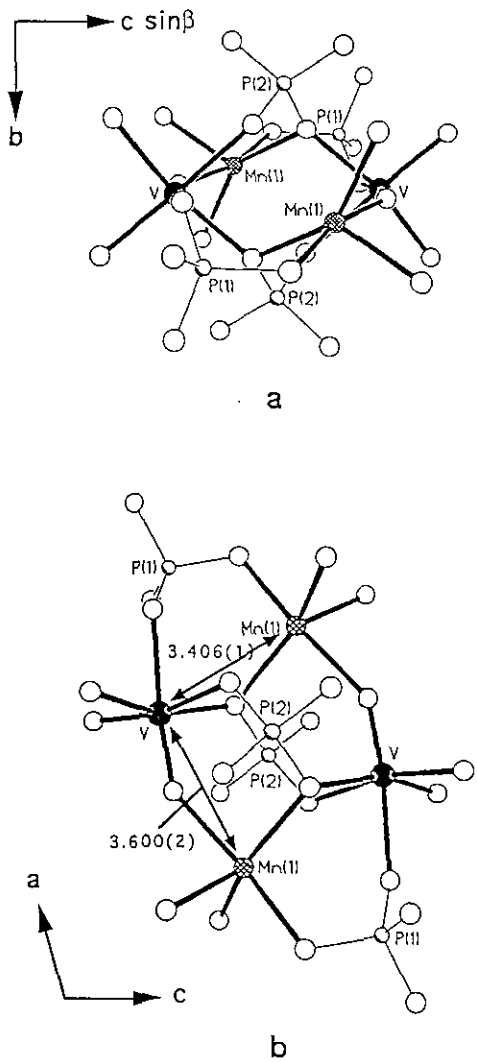

FIG. 2. The cyclic tetrameric cluster of $Mn(1)O_5$ polyhedra and VO_6 octahedra in $Mn_2VO(PO_4)_2 \cdot H_2O$, viewed (a) along the edge (along *a*), and (b) perpendicular to the face (along *b*). PO_4 tetrahedra straddle the edges and span the faces of the cluster. The metal–metal distances within the cluster are indicated.

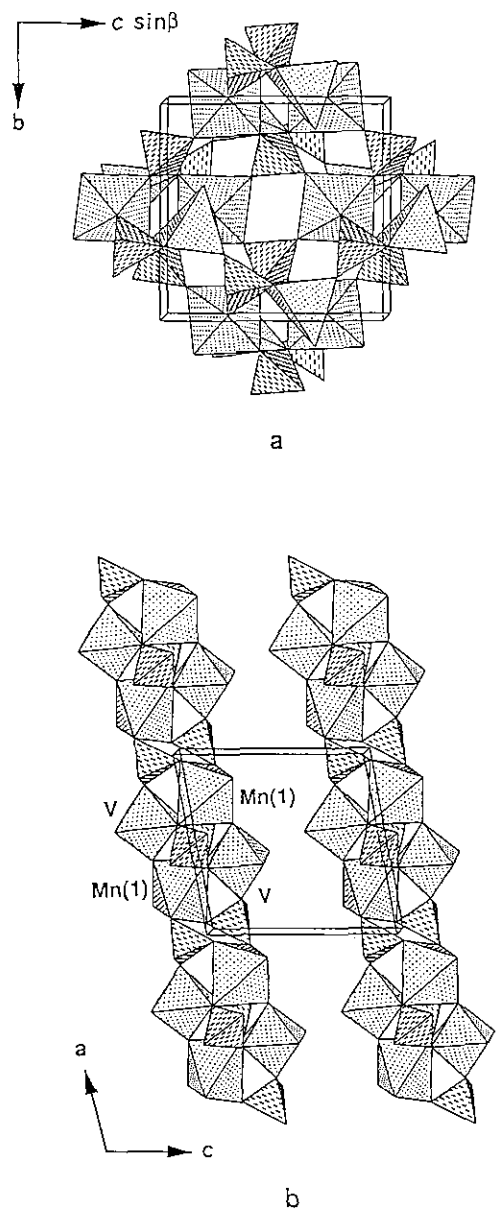

FIG. 3. Polyhedral representation of the linkage of the tetrameric Mn(1)–V clusters in $Mn_2VO(PO_4)_2 \cdot H_2O$, with cell outline shown. The $Mn(1)O_5$ polyhedra and VO_6 octahedra are dotted, and the PO_4 tetrahedra are dashed. Viewed along *a*, four clusters are linked together through the PO_4 tetrahedra, forming cavities at the center and origin of the unit cell. (b) Viewed along *b*, the clusters located at the section $y = 1/2$ are linked to form chains running along the [100] direction. For clarity, the section $y = 0$ is not shown in this view.

cluster and by $P(2)O_4$ tetrahedra above and below the plane of the cluster. In so doing, the metal polyhedra must tilt toward each other to accommodate the short P–O bonds of the PO_4 tetrahedra, resulting in metal–metal distances of 3.406(1) and 3.600(2) Å within the cluster.

Successive clusters are linked together end-to-end by the $P(1)O_4$ tetrahedra, forming columns running along the [100] direction and lying parallel to the (010) plane at $y = 0$ and 1/2 (Fig. 3). The columns are then joined together to neighboring columns (related by the *c*-glide plane $y = \pm 1/4$) in adjacent planes translated $\pm 1/2$ along the *b* direction by both $P(1)O_4$ and $P(2)O_4$ tetrahedra, forming a three-dimensional framework.

Up to this point, the Mn(1) and V polyhedra have remained isolated within the tetrameric clusters, which are separated by PO_4 tetrahedra. The Mn(2) polyhedra is now introduced into the framework to yield the complete structure (Fig. 4). It provides an additional link between clusters belonging to neighboring columns, corner-sharing with a $Mn(1)O_5$ polyhedron of one cluster and edge-sharing with a VO_6 octahedron of another cluster. Including the long Mn(2)–O(9) bond results in two octahedra

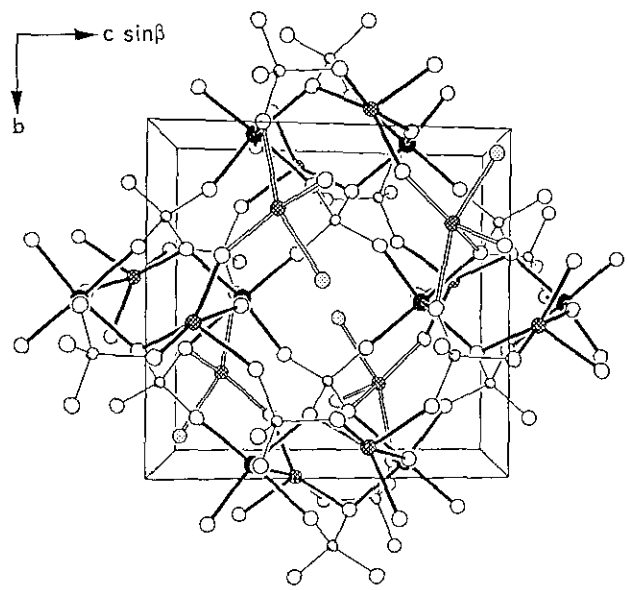

FIG. 4. View along the a direction of the complete structure of $Mn_2VO(PO_4)_2 \cdot H_2O$, with cell outline shown and with the $Mn(2)O_5$ polyhedra now included. The hatched circles are Mn atoms, the solid circles are V atoms, the partly shaded circles are P atoms, and the open circles are O atoms; the dotted circles are O(8) atoms, which are part of water molecules. The bonds in the $Mn(1)O_5$ polyhedra and VO_6 octahedra forming the tetrameric clusters are solid, those in the $Mn(2)O_5$ polyhedra are open, and those in the PO_4 tetrahedra are thin lines.

$Mn(2)O_6$ and VO_6 sharing a common face, with the Mn(2)–V distance being 3.150(2) Å (Fig. 1c). The O(8) atom belonging to the water molecule points in toward the cavity (x, 0, 0 or x, 1/2, 1/2) defined by the assembly of clusters. Although there are several O(8)–O distances across the cavity that are less than 3.0 Å (e.g., O(8)–O(3), 2.866(6); O(8)–O(9), 2.902(6); O(8)–O(8) in the next unit cell, 2.974(8) Å), the question whether hydrogen bonding exists remains open, for the protons could not be located.

Magnetism. Magnetic measurements were conducted on $Mn_2VO(PO_4)_2 \cdot H_2O$ in order to confirm the assignment of metal oxidation states. Figure 5 shows a plot of the reciprocal magnetic susceptibility vs temperature for $Mn_2VO(PO_4)_2 \cdot H_2O$. The compound displays Curie–Weiss behavior down to T_N = 20 K, at which point an antiferromagnetic transition takes place. The high temperature portion (150–300 K) was fit to the Curie–Weiss expression, yielding a Curie constant of C = 9.0 emu K^{-1} $mole^{-1}$ and a Weiss constant of $\theta = -46$ K. The effective magnetic moment μ_{eff} = 8.5 BM is in excellent agreement with the spin-only value expected for a system consisting of two isolated high-spin Mn^{2+} ions (S = 5/2) and one isolated V^{4+} ion (S = 1/2), μ_{so} = 8.54 BM, and rules out other possible assignments of oxidation states. Examination of the metal–metal distances in the structure reveals that most of them are too long for any direct coupling interactions to be significant; within the tetrameric cluster depicted in Fig. 2b, the Mn(1)–V distances are greater than 3.4 Å. The origin of the antiferromagnetic interaction most likely arises between the Mn(2) and V atoms (Fig. 1c), which are 3.150(2) Å apart in their edge-sharing polyhedral arrangement (or, alternatively viewed, face-sharing octahedral arrangement).

Thermal behavior. Thermal gravimetric analysis shows that $Mn_2VO(PO_4)_2 \cdot H_2O$ decomposes at 400°C. The O–H stretching and bending vibrations, centered at 3400 and 1620 cm^{-1}, respectively, in the infrared spectrum, disappear in a sample heated to 500°C. The X-ray powder pattern of the heated sample is considerably different and rather simplified compared to that of $Mn_2VO(PO_4)_2 \cdot H_2O$, implying that radial changes in the structure have occurred upon decomposition. Further characterization of this nominally dehydrated phase is in progress.

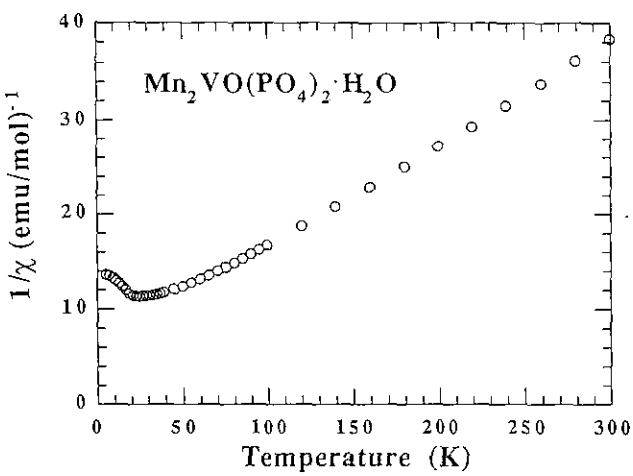

FIG. 5. Plot of reciprocal magnetic susceptibility vs temperature for $Mn_2VO(PO_4)_2 \cdot H_2O$.

ACKNOWLEDGMENTS

We thank Dr. C. Payen for the magnetic susceptibility measurement. A. M. thanks NSERC Canada for financial support in the form of a postdoctoral fellowship.

REFERENCES

1. L. Benes, K. Richtrova, J. Votinsky, J. Kalousova, and V. Zima, *Powder Diffr.* **8,** 130 (1993).
2. G. Centi, F. Trifiro, J. R. Ebner, and Y. M. Franchetti, *Chem. Rev.* **88,** 55 (1988).
3. M. Uchiyama, S. Slane, E. Plichta, and M. Salomon, *J. Electrochem. Soc.* **136,** 36 (1989).
4. M. Tsuji, S. Komarneni, Y. Tamaura, and M. Abe, *Mater. Res. Bull.* **27,** 741 (1992).

5. F. Leroux, A. Mar, C. Payen, D. Guyomard, A. Verbaere, and Y. Piffard, *J. Solid State Chem.*, in press.
6. K. Yvon, W. Jeitschko, and E. Parthé, *J. Appl. Crystallogr.* **10,** 73 (1977).
7. Sheldrick, G. M., "SHELXTL PLUS 4.0," Siemens Analytical X-Ray Instruments, Inc., Madison, WI, 1990.
8. D. T. Cromer and J. T. Waber, *in* "International Tables for X-Ray Crystallography," Vol. IV, Tables 2.2B and 2.3.1, Kynoch Press, Birmingham, England, 1974.
9. N. E. Brese and M. O'Keeffe, *Acta Crystallogr. Sect. B* **47,** 192 (1991).
10. I. D. Brown and D. Alatermatt, *Acta Crystallogr. Sect. B* **41,** 244 (1985).